Distributed Model Predictive Control of Centrifugal Compressor Systems

K. Jones * **A. Cortinovis** * **M. Mercangoez** *

* *ABB Switzerland Ltd., Corporate Research, Baden-Dättwil, Switzerland (e-mail: katie.jones@reactive-robotics.com, andrea.cortinovis@ch.abb.com, mehmet.mercangoez@ch.abb.com).*

Abstract: The performance and computational cost of distributed MPC for the control of compressor networks is investigated in simulation. Both cooperative and non-cooperative approaches are considered and compared to the performance achieved with centralized control in the presence of a discharge-side disturbance. Two systems, each with two compressors, are studied: one is arranged in parallel configuration and the other in series. Due to the high degree of non-linearity of both systems, the models are re-linearized at each time step and a linear, delta MPC formulation is used. The controller is implemented using the quadratic program solver `qpOASES`. The non-cooperative controller exhibited a significantly reduced computation time relative to the centralized controller (25% and 40% lower for the parallel and serial configurations, respectively), while the cooperative controller did not significantly reduce the computation time. For the parallel configuration, both distributed and centralized controllers had identical control performance. For the serial configuration, only the cooperative controller achieved similar performance to the centralized approach; the non-cooperative controller demonstrated a 9% reduction in the minimum surge control distance reached in the downstream compressor.

Keywords: Distributed mpc, anti-surge control, nonlinear mpc, compressor modeling, variable speed drive

1. INTRODUCTION

Centrifugal gas compressors are employed in a wide range of industrial applications, particularly for gas transportation, extraction and processing. Compression is an inherently energy-intensive process, with well over 90% of operating costs spent on energy; small improvements in efficiency can therefore have a significant impact on the operating costs. At the same time, compressors are critical components in natural gas installations, meaning even short downtimes can also have a large economic impact. Compressor control systems must therefore maintain the compressor's operating point within its safe operating regime, avoiding instabilities that may damage its machinery and lead to such downtimes. The most relevant of these instabilities for control is surge, a phenomenon that occurs when the pressure ratio across the compressor is too high for the mass flow, leading to oscillations in mass flow and output pressure, as well as vibrations and an increase in temperature. Surge can cause permanent damage to machinery in a relatively short time span and it is imperative for industrial compressor control systems to avoid it.

Compressor control thus consists of two sometimes competing goals: process control, wherein a variable (e.g. output pressure) is maintained at a reference value, and anti-surge control (ASC), which keeps the compressor out of the surge regime. The performance of a compressor's anti-surge controller (ASC) is relevant for its efficiency: the most efficient operating points often lie on or near the surge line bounding the unstable surge regime. Controllers that allow the compressor to be operated closer to surge thus lead directly to an increase in the attainable efficiency.

The current state-of-the-art in compressor control uses two independent controllers for process control and ASC. The process controller operates by manipulating the speed of the gas turbine or electric driver driving the compressor, while the ASC keeps the compressor away from surge by manipulating the position of a recycle valve. This valve can be opened to allow flow from the outlet back to the inlet, effectively increasing the mass flow of the compressor and decreasing its pressure ratio, moving the system away from surge. These controllers are currently implemented using simple PID controllers, with added loop decoupling and hand-tuned open-loop control responses near boundaries to address nonlinearities and control interactions. Constraints are generally treated using clipping and anti-windup logic, which require further tuning.

Such a decoupled approach is necessary when considering gas turbine-powered compressors, as the dynamics of the turbine are much slower than those that lead to compressor surge. The transition of compressor control from gas turbines to electric drivers with faster torque responses has, however, opened the door for new, multivariable control algorithms that combine process control and ASC into a single controller. Such a multivariable controller can take advantage of the quick response of electric driver torque compared to the recycle valve opening to decrease

the response time of the ASC to disturbances, thereby increasing its performance.

In recent years, model predictive control (MPC) has been proposed as an alternative to frequency-domain approaches as it can explicitly consider both the coupling and physical constraints that make compressor control so challenging. Cortinovis et al. showed that combined process and ASC using MPC led to a reduced distance to surge and a reduced settling time for process control in a centrifugal compressor in experiments compared to the current state-of-the-art Cortinovis et al. (2015). Similarly, Budinis and Thornhill found that a combined process/ASC MPC controller better handled disturbances and changes in load pattern compared to a PID controller in simulation Budinis and Thornhill (2015). Bentaleb et al. also demonstrated that an MPC controller manipulating driver speed and the inlet guide vanes could achieve better process performance than a PID controller manipulating only the driver speed Bentaleb et al. (2014). This result was extended by Bentaleb to include the use of a recycle valve to combine process and anti-surge control Bentaleb (2015).

The major disadvantage of MPC compared to conventional control approaches is its computational complexity, and the resulting difficulty of achieving a sampling rate fast enough to handle the relatively fast dynamics observed in compressors. Furthermore, in industrial applications, compressors are often combined, either in parallel to increase mass flow, or in series to increase the pressure ratio achieved. In such systems, as the number of states and inputs increase so does the required computation time of an MPC controller, making traditional MPC impractical in many situations.

In this article a distributed MPC (dMPC) control approach is proposed, which overcomes this limitation by dividing the optimization problem posed by a multi-compressor system into sub-problems to be solved at the individual compressor level. These sub-problems can be solved in parallel, reducing the required sample time as compared to a centralized MPC solution. Two variants of dMPC are examined: a cooperative scheme where each compressor optimizes a single cost function using its own inputs, and a non-cooperative scheme where each compressor optimizes a cost function based only on its own inputs and outputs.

The use of dMPC implies a loss of performance compared to a traditional, centralized MPC controller. This loss – in particular for ASC performance – are examined for both the cooperative and non-cooperative control approaches. In addition to the controller performance, the computational efficiency of each control approach is evaluated. Two compressor systems are considered as test cases to evaluate the performance of the dMPC approach in simulation: a parallel and a serial configuration, each with two compressors.

2. MODELLING & SIMULATION

The models used in this work are based on a two-compressor system at an ABB Research facility. The physical setup is described in Cortinovis et al. (2015) for a

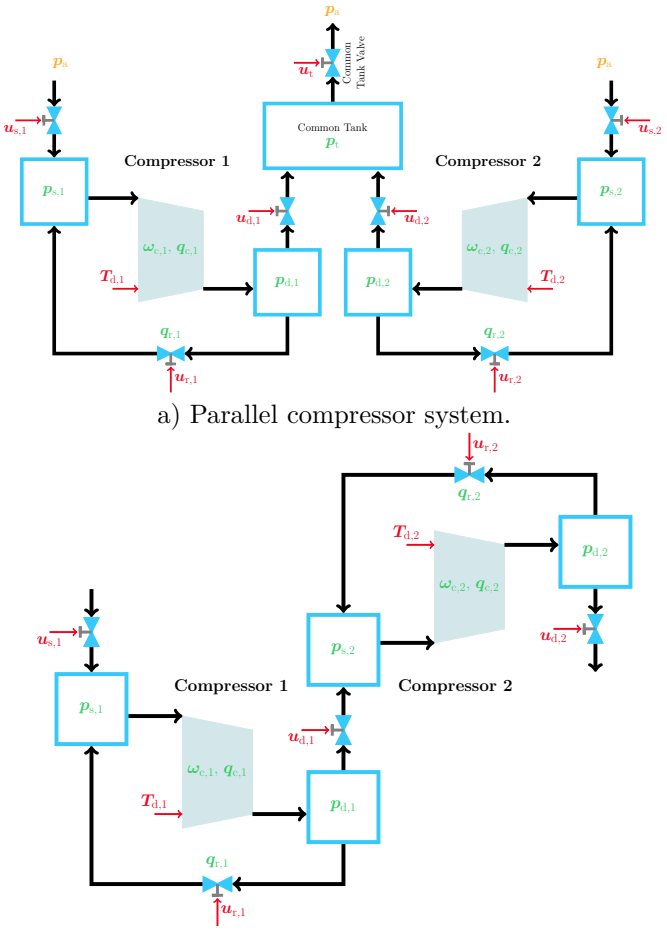

a) Parallel compressor system.

b) Serial compressor system.

Fig. 1. Diagram of compressor systems with inputs and states labelled.

single compressor. For simplicity, the two compressors in each system were assumed to be identical.

The compressor model used in this work is a centrifugal compressor driven by a variable-speed electric driver, with a tank at both the inlet (suction) and outlet (discharge). Both the suction and discharge tanks are connected to atmospheric pressure by a valve. These suction and discharge valves represent the flow conditions upstream and downstream of the compressor, such that various flow conditions and disturbances can be simulated by changing the position of the valves. The artificial disturbances applied using these valves are designed to mimic situations frequently encountered in industrial applications (e.g. shutdown or startup of a downstream compressor). The compressor model used is based on the Gravdahl-Greitzer model described in Gravdahl and Egeland (1999). It is defined by five states: the suction (p_s) and discharge (p_d) pressures, the mass flow through the compressor (q_c), the rotational speed of the compressor (ω_c), and the mass flow rate through the recycle valve (q_r). The two inputs to the system are the torque applied to the electric driver (T_d) and the position of the recycle valve (u_r). The controlled outputs are the output pressure (p_out) and the surge distance (SD), a measure of how far the compressor is from surge. The interested reader may refer to Cortinovis et al. (2015) for a more detailed description of the model and its identification.

The parallel and serial compressor systems studied in this work are shown in Figure 1. In the parallel case, the two compressors' outlet tanks both discharge into a single discharge tank and the pressure in this discharge tank (p_t) is the primary process variable. This pressure also serves as an additional state while the inputs and outputs remain the same as for a single compressor. For the serial configuration, the upstream compressor discharges directly into the inlet of the downstream compressor. The states, inputs and outputs are the same as those of the individual compressors.

3. MODEL PREDICTIVE CONTROL FORMULATION

Two variants of MPC are considered in this work: centralized and distributed control. Centralized control is considered too computationally expensive to implement in practice, but it is used as a benchmark to evaluate the performance of the distributed controllers. The system considered is non-linear, however, in order to take advantage of efficient quadratic program (QP) solvers, the non-linear system is re-linearized at each time step and the resulting linear model used to generate the optimization. In order to control the relatively fast dynamics leading to compressor surge, the controllers operate at a sampling rate of $t_\mathrm{s} = 50\,\mathrm{ms}$. The model used for the MPC controller formulation is the same as the one used in Section 2 to simulate the compressor. No model mismatch was considered in order to compare the controllers' performance in an ideal scenario.

The nonlinear model is linearized at each sampling instant about the current states ($\hat{\boldsymbol{x}}_k$) and inputs ($\boldsymbol{u}_{k-1}$), and discretized using the 4th order Runge-Kutta method. The resulting discrete-time, linear system is then augmented to include both error states as integrators for offset-free control, and delayed input states for the recycle valve. One integrator for each output is added, as well as 40 delayed states per compressor (giving a total delay of 2 s). The interested reader may refer to Jones (2016) for a detailed development of the augmented state equations.

Based on the linearized, augmented model, the optimization problem solved at each time step is defined as follows:

$$\begin{aligned} U_k = \arg\min_{U} \; & \Delta U^\intercal \; Q \; \Delta U \\ & + \left(\Delta Y - \Delta Y_k^\mathrm{ref}\right)^\intercal R \left(\Delta Y - \Delta Y_k^\mathrm{ref}\right) \\ \text{s.t. } & \Delta U_\mathrm{min} \leq \Delta U \leq \Delta U_\mathrm{max} \\ & \Delta U_\mathrm{r,min} \leq A_\mathrm{rate} \Delta U \leq \Delta U_\mathrm{r,max} \\ & \Delta Y_k = S_{U_k} \Delta U_k + S_{x_k} \Delta \hat{\boldsymbol{x}}_k^a + S_{f_k} \boldsymbol{f}_{\mathrm{d},k}, \end{aligned} \tag{1}$$

where:

- U_k contains the optimal input sequence at time step k, stacked along the move horizon m;
- Y_k contains the output sequence resulting from the input sequence U_k at time step k, stacked along the prediction horizon p;
- Y_k^ref is the reference output sequence;
- Q and R are the weighting matrices used for the inputs and outputs, respectively;
- S_{U_k}, S_{x_k} and S_{f_k} are the prediction matrices giving the contribution to ΔY_k of ΔU_k, $\Delta \hat{\boldsymbol{x}}_k^a$ and $\boldsymbol{f}_{\mathrm{d},k}$ respectively;
- ΔU_min, ΔU_max, $\Delta U_\mathrm{r,min}$ $\Delta U_\mathrm{r,max}$ contain the input bounds and rate constraints; and
- A_rate is a matrix that is multiplied by ΔU_k to obtain the changes in inputs between two successive time steps.

The optimization is then converted to a dense formulation by eliminating the dependence on ΔY_k through the equality constraint, and expressed as a QP problem with Hessian and linear terms dependent on the type of controller used.

The prediction horizon p used was 100, giving a prediction of 5 s determined to be sufficient to capture the relevant compressor dynamics. To decrease the aggressiveness of the controller as well as the QP complexity, a lower move horizon m of 2 was used.

The input constraints are determined by combining limits on both the range of the inputs and on their rate of change. The recycle valve has a range of 0–1 with rate constraints (maximum possible change over a single sampling period) of +1/-0.1. The rate is more constrained in the negative direction (i.e. when closing) to prevent a transient reentry into surge. The torque input has a normalized range of ± 0.3 compared to its steady-state value, with rate constraints of ± 0.1.

3.1 Centralized MPC

In the centralized control approach, a single MPC controller is used to optimize for all system inputs using a single cost function with quadratic weights on inputs and outputs. At each sampling period, the optimal input is computed using the following algorithm:

(1) perform estimation to obtain the current estimate of the augmented state vector;
(2) linearize, discretize and augment non-linear model about the current state estimate and previous inputs;
(3) generate the prediction matrices using the augmented state equations;
(4) set up the QP problem and solve using the `qpOASES` solver;
(5) apply the optimal input at the first prediction interval to the system.

The QP formulation for the centralized controller is given by:

$$\begin{aligned} H &= 2\left(Q + S_{U_k}^\intercal \; R \; S_{U_k}\right) \\ g &= 2\left(\Delta \hat{\boldsymbol{x}}_k^a S_{x_k}^\intercal + \boldsymbol{f}_{\mathrm{d},k} S_{f_k}^\intercal - \Delta Y_k^\mathrm{ref}\right) R S_{U_k}. \end{aligned} \tag{2}$$

The centralized controller assigns weights to each input and controlled output. For the parallel system, the controlled outputs are the surge distances of both compressors as well as the pressure of the common tank. A fourth output could be added to account for load sharing, but was not considered in this work since the compressors were assumed to be identical. For the serial system, the controlled outputs are the surge distances and output pressures of both compressors.

3.2 Distributed MPC

In the distributed MPC approach, the control problem is split into two smaller optimizations, each giving the optimal input for a single compressor. The two sub-controllers are assumed to have full state information and the optimizations are set up as QPs, as for the centralized controller, with an identical Hessian (H) term. A slight modification to the linear term is necessary to account for the fact that the QP is solved for only part of the optimal input vector:

$$g_{\text{distributed}} = g_{\text{centralized}} + \Delta U_k^{\text{ot}} \; S_{U_k^{\text{ot}}}^{\mathsf{T}} R \; S_{U_k} \qquad (3)$$

where U_k^{ot} is the optimal input calculated by the other sub-controller, and $S_{U_k^{\text{ot}}}$ is the prediction matrix giving the effect of the other sub-controller's inputs on the current outputs ΔY_k.

This QP is unsolvable since U_k^{ot} in turn depends on its solution. To break this circular dependency, the problem is initially solved with an estimate for U_k^{ot} obtained from the previous QP solution. The sub-controllers then exchange their obtained solutions and re-solve the optimization. This procedure is repeated for a fixed number of iterations. [1]

The algorithm used to obtain the optimal input at each time step for a distributed controller is thus the same as for the centralized controller, with the exception that the QP is solved iteratively with information exchange between the controllers. The number of solver iterations used in this work was fixed at 3, based on an analysis of the cost function evolution as a function of solver iterations, which improves only marginally after 3 iterations. The details of this analysis are presented in Jones (2016).

The cost functions used by the dMPC controllers apply weights to only a subset of the inputs and outputs. For the cooperative controllers, all sub-controllers have equal weights on all outputs, but only have weights applied to the inputs of their corresponding compressor. For the non-cooperative controllers, the sub-controllers have non-zero weights on the inputs and outputs of their compressor.

4. SIMULATION RESULTS

In order to test the controller performance of the various control implementations, a single benchmark disturbance case was chosen. It is designed to mimic a typical disturbance downstream of the system such as the shutdown of another compressor. The disturbances used were as follows:

- **parallel**: common tank discharge valve (u_{t}) 70% -> 40% open;
- **serial**: downstream compressor discharge valve ($u_{\text{d},2}$) 39% -> 29% open.

In the following plots, the disturbances are persistent and applied at 50 s, after the system has reached steady state.

[1] The iteration process may not converge for systems that have a high degree of coupling; this effect is discussed in further detail in Stewart et al. (2010).

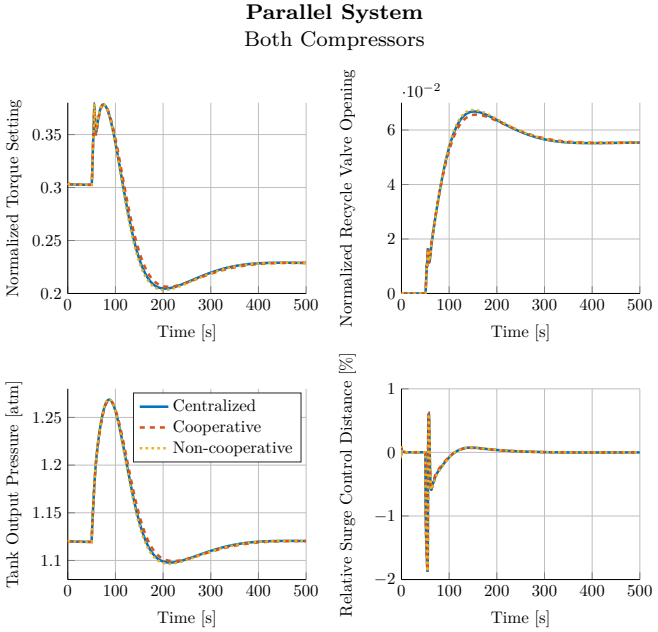

Fig. 2. Comparison of time responses of centralized and distributed controllers using 3 solver iterations. Output disturbance is applied at 50 s.

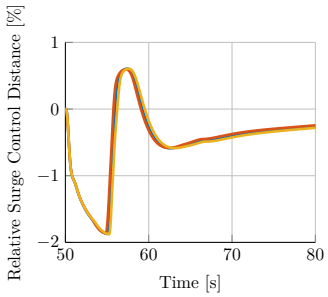

Fig. 3. Zoomed view of surge distance time response given in Figure 2.

The distributed controllers in this section were implemented using 3 controller iterations. As discussed in Jones (2016), this number was determined sufficient for convergence of the applied inputs.

4.1 Parallel System Control Performance

The time response of each controller for the parallel system is shown in Figure 2. The responses obtained using each of the three controllers are virtually identical – in this case, using a distributed control approach has no performance penalty and a potential decrease in computational cost (see below).

The integral squared error (ISE) and integral absolute error (IAE) are shown in Table 2 for all controllers.

4.2 Serial System Control Performance

The time response of the serial system is shown in Figure 4. A zoomed view of the initial surge distance response is shown in Figure 5.

Differences in the controller response and performance can be observed for each of the control approaches. The

Table 1. Integral squared error (ISE) and integral absolute error (IAE) measures for parallel controllers.

	Centralized		Cooperative		Non-cooperative	
	ISE	IAE	ISE	IAE	ISE	IAE
T_d	0.0026	0.027	0.0026	0.028	0.0026	0.028
u_r	0.00012	0.0057	0.00011	0.0056	0.00012	0.0059
SD	0.035	0.057	0.033	0.054	0.036	0.059
p_t	0.0023	0.025	0.0024	0.026	0.0023	0.025

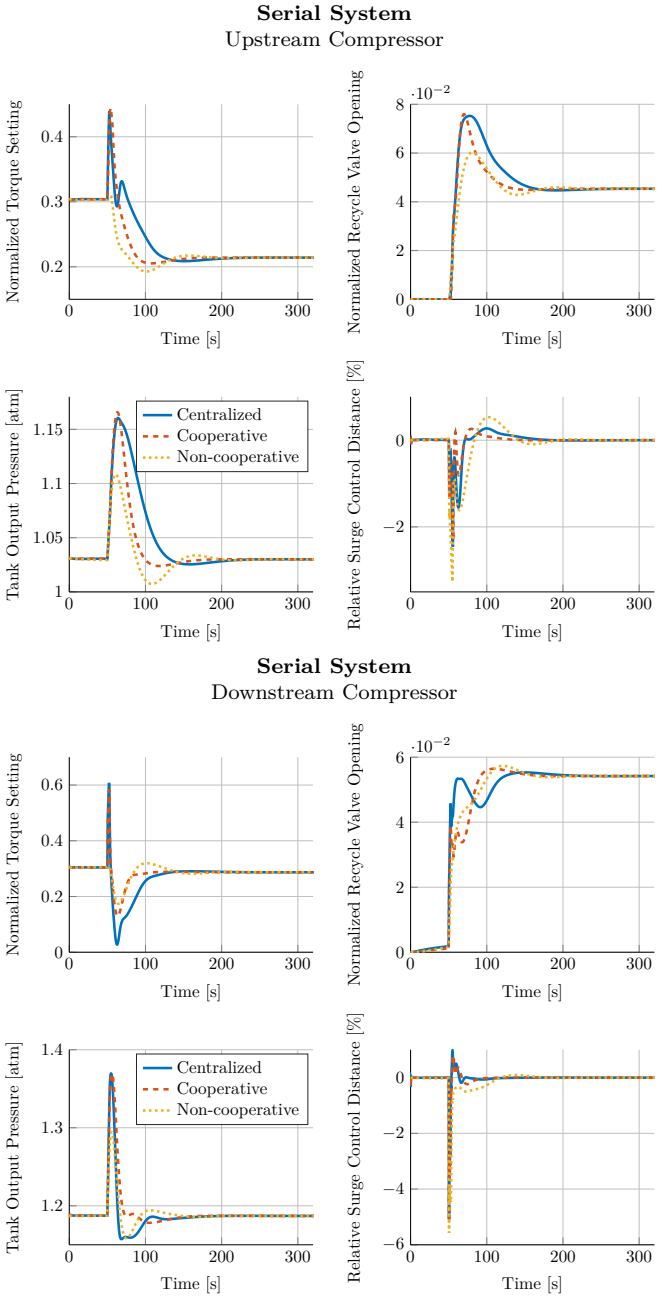

Fig. 4. Comparison of time responses of centralized and distributed controllers using 3 solver iterations. Output disturbance is applied at 50 s.

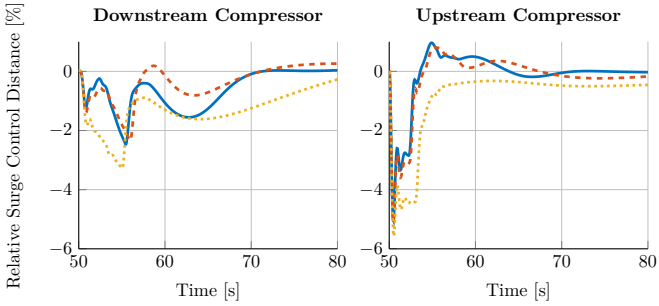

Fig. 5. Zoomed view of surge distance time response given in Figure 4.

Table 2. Integral squared error (ISE) and integral absolute error (IAE) measures for serial controllers.

	Centralized		Cooperative		Non-cooperative	
	ISE	IAE	ISE	IAE	ISE	IAE
$T_{\mathrm{d},1}$	0.0012	0.012	0.001	0.0079	0.0015	0.019
$u_{\mathrm{r},1}$	8.6e-05	0.0037	5.6e-05	0.0024	0.00011	0.0053
$p_{\mathrm{d},1}$	0.00096	0.011	0.0006	0.0067	0.00081	0.014
SD_1	0.052	0.063	0.031	0.041	0.078	0.13
$T_{\mathrm{d},2}$	0.0027	0.016	0.00095	0.0073	0.0017	0.021
$u_{\mathrm{r},2}$	1.1e-05	0.0011	2.7e-05	0.0016	3.2e-05	0.0026
$p_{\mathrm{d},2}$	0.00047	0.0051	0.00058	0.0049	0.00029	0.005
SD_2	0.056	0.032	0.064	0.035	0.1	0.064

cooperative controller response is qualitatively similar to that of the centralized controller. It is, however, somewhat less aggressive in its regulation of the output pressure, evidenced by its less extreme change from high to low torque in the downstream compressor and faster return to the steady-state torque value, as shown in Figure 4. As a result, the output pressure of the downstream compressor has a much lower overshoot than either the centralized or non-cooperative controller. The surge distances of the centralized and cooperative controllers, however, show an almost identical response for the downstream compressor and a similar response upstream, though that of the cooperative controller has a greater increase near 58 s (see Figure 5).

The non-cooperative controller response has a much different characteristic than that of the centralized controller. There is no significant initial increase in the torque input to either compressor when the disturbance is applied; as a result, both compressors are pushed further towards surge than in the centralized or cooperative case, and the surge distances are also slower to converge. The maximum disturbance to the output pressures of both compressors for the non-cooperative controller is accordingly reduced by approximately 40% when compared to the centralized case.

The integral squared error (ISE) and integral absolute error (IAE) are shown in Table 2 for all controllers.

4.3 Computational Efficiency

The computational cost of the centralized and distributed control approaches was evaluated and is presented in

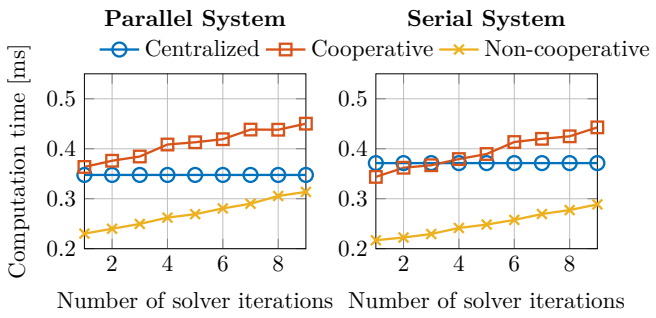

Fig. 6. Average controller computation time per iteration, as a function of the number of solver iterations used. Operating point is 3 solver iterations. Output disturbance is applied at 50 s and total simulation time is 500 s.

Figure 6. [2] The computation times for the distributed controllers assume a parallelized implementation where each sub-controller is executed using a separate processor.

As expected, the non-cooperative controller achieves the lowest computation times for both the parallel and the serial system. In both cases, the cooperative controller has a computation time approximately on par with the centralized controller.

The significant advantage in computation time demonstrated by the non-cooperative controller is a result of the reduced size of its prediction matrices, which are multiplied to generate the QP. The computational cost of the QP generation is approximately linear in the number of outputs used, and the non-cooperative approach considers fewer outputs than the centralized or cooperative approaches.

As described in Jones (2016), for the systems considered here, the QP-generation step has a much higher computational cost than the QP-solving step. There is thus limited scope for decreasing the required computation time without decreasing the number of states used to generate the QP problem.

5. CONCLUSION

In this work, the development of a distributed model predictive control scheme combining process and anti-surge control for systems of compressors was presented. Two compressor networks were studied: a parallel and a serial configuration, each with two compressors. The control scheme was based on linearized MPC using a linear model of the system updated at each time step. Distributed controllers using both cooperative and non-cooperative cost functions were developed.

The performance of the distributed controllers was then evaluated in simulation and compared to the benchmark established by a centralized MPC controller. For the parallel system, both cooperative and non-cooperative controllers achieved virtually identical control performance to the centralized controller. The cooperative controller had a 11% higher average computation time than in the centralized case, while the non-cooperative scheme reduced the average computation time by 28%.

[2] Tests run on a Intel® Core™ i5-540M 2.53 GHz processor.

The serial system had different controller performances for each of the centralized, cooperative and non-cooperative controllers. The cooperative controller achieved very similar performance in the time response as the centralized controller, with $< 1\%$ difference in both the maximum discharge pressure and minimum surge control distance in the downstream compressor. The non-cooperative controller also had a qualitatively similar response, however it did not perform as well in anti-surge control, with a 9% decrease in the minimum surge control distance reached in the downstream compressor compared to the centralized controller. Its reduced performance in surge control was combined with improved process control: its maximum discharge pressure was 40% lower than in the centralized case. Again, the non-cooperative controller outperformed the cooperative controller in terms of computation time, giving a 38% decrease compared to the centralized case, while the cooperative controller only achieved a 1% reduction.

The computational efficiency of the distributed controllers could be further improved by investigating the effect of reducing the model order at the sub-controller level on overall controller performance. In particular, reducing the number of states used to generate the prediction matrices could lead to relatively high performance gains as the prediction matrix generation is $\mathcal{O}(n^3)$ in the number of states.

REFERENCES

Bentaleb, T. (2015). *Model-Based Control Techniques for Centrifugal Compressors.* Ph.d thesis, University of Siena. doi:10.13140/RG.2.1.2265.2965.

Bentaleb, T., Cacitti, A., De Franciscis, S., and Garulli, A. (2014). Multivariable control for regulating high pressure centrifugal compressor with variable speed and IGV. In *2014 IEEE Conference on Control Applications, CCA 2014*, 486–491. Antibes, France. doi:10.1109/CCA.2014.6981393.

Budinis, S. and Thornhill, N. (2015). Control of centrifugal compressors via model predictive control for enhanced oil recovery applications. In *IFAC Workshop on Automatic Control in Offshore Oild and Gas Production*, volume 48, 9–14. Elsevier Ltd., Florianopolis, Brazil. doi:10.1016/j.ifacol.2015.08.002.

Cortinovis, A., Ferreau, H., Lewandowski, D., and Mercangöz, M. (2015). Experimental evaluation of MPC-based anti-surge and process control for electric driven centrifugal gas compressors. *Journal of Process Control*, 34, 13–25. doi:10.1016/j.jprocont.2015.07.001.

Gravdahl, J.T. and Egeland, O. (1999). Compressor Surge and Stall: An Introduction. In *Compressor Surge and Rotating Stall*, 1–62. Springer London.

Jones, K. (2016). *Distributed model predictive control of compressor systems.* Master's thesis, Ecole polytechnique fédérale de Lausanne.

Stewart, B.T., Venkat, A.N., Rawlings, J.B., Wright, S.J., and Pannocchia, G. (2010). Cooperative distributed model predictive control. *Systems and Control Letters*, 59(8), 460–469. doi:10.1016/j.sysconle.2010.06.005.